Structure and function of tomato disease resistance proteins

van Ooijen, G.

Publication date
2008

Chapter 4

Transcomplementation, but not physical association of the CC-NB-ARC and LRR domains of tomato R protein Mi-1.2 is altered by mutations in the ARC2 subdomain

Gerben van Ooijen, Gabriele Mayr[1], Mario Albrecht[1], Ben J. C. Cornelissen and Frank L. W. Takken

[1] Max Planck Institute for Informatics, Saarbrücken, Germany
Published in: Molecular Plant, 2008, Volume 1, 401-410

Race-specific disease resistance in plants is mediated by Resistance (R) proteins that recognise pathogen attack and initiate defence responses. Most R proteins contain a central NB-ARC domain and a C-terminal leucine-rich repeat (LRR) domain. We analysed the intramolecular interaction of the LRR domain of tomato R protein Mi-1.2 with its N-terminus. We expressed the CC-NB-ARC and LRR parts *in trans* and analysed functional transcomplementation and physical interactions. We show that these domains functionally transcomplement when expressed *in trans*. Known autoactivating LRR domain swaps were found to induce a hypersensitive response (HR) upon co-expression *in trans*. Likewise, autoactivating mutants in the NB subdomain transcomplemented to induce HR. Point mutations in the ARC2 subdomain that induce strong autoactivation in the full-length Mi-1.2 protein, however, fail to induce HR in the transcomplementation assay. These data indicate distinct functions for the three NB-ARC subdomains in induction of HR signalling. Furthermore, dissociation of the LRR is not required to release its negative regulation, as in all combinations of CC-NB-ARC and LRR domains tested a physical interaction was observed.

Introduction

Race-specific resistance in plants is mediated by specific surveillance proteins called resistance (R) proteins (Tameling and Takken, 2007). Upon pathogen perception, R proteins trigger a strong defence response often culminating in a hypersensitive response (HR), a form of programmed cell death mechanism aimed at restricting pathogen proliferation. Most R proteins are large intracellular proteins that contain a central Nucleotide Binding (NB-) domain fused to a C-terminal leucine-rich repeat (LRR) domain.

The LRR domain consists of a variable number of leucine-rich repeat units and harbours negative as well as positive regulatory functions. The positive regulatory role for R protein function is apparent as the LRR domain is indispensable and deletion normally does not result in constitutive activity (Bendahmane et al., 2002; Hwang and Williamson, 2003; Rathjen and Moffett, 2003). The negative regulatory function becomes clear when an LRR is improperly matched to the rest of an R protein. For instance, swapping the Mi-1.2 LRR region into paralogue Mi-1.1 results in autoactivity, i.e. activation of defence responses in the absence of the pathogen. The reciprocal swap results in loss of nematode resistance in transgenic roots (Hwang et al., 2000). Likewise, autoactivation upon LRR exchange has been observed for maize Rp1 homologues (Sun et al., 2001) and by swapping parts of the potato Rx LRR domain for the corresponding (highly homologous) Gpa2 sequences (Rairdan and Moffett, 2006). These experiments suggest that the LRR domain interacts with the rest of the protein and that improper pairing can result in de-repression of the protein. Direct physical and functional interaction of the R protein LRR domain with the rest of the protein has indeed been shown, first for potato Rx (Moffett et al., 2002) and later for tobacco N (Ueda et al., 2006), pepper Bs2 (Leister et al., 2005) and *Arabidopsis* RPS5 (Ade et al., 2007). Altogether, these observations indicate that subtle intramolecular interactions between the LRR domain and the N-terminus are required for proper R protein function.

The most well-conserved protein domain in NB-LRR proteins is the NB-ARC domain. This nucleotide-binding domain is found in proteins such as human Apaf-1, plant R proteins and *C. elegans* Ced-4 (ARC), hence its name NB-ARC. When the crystal structures of NB-ARC domains were established for Apaf-1 and CED-4 (Riedl et al., 2005; Yan et al., 2005), it became apparent that the NB-ARC consists of structurally defined subdomains. No plant NB-ARC domain has been crystallised so far, but based on homology modelling it has been proposed that the R protein NB-ARC consists of three subdomains; a nucleotide-binding fold (NB), a four-helix bundle (ARC1) and a winged-helix fold (ARC2) (Albrecht and Takken, 2006). These subdomains are spatially well-defined and are proposed to have functionally distinct roles, as elaborated below. The NB-ARC domain of R proteins I-2, Mi-1 and N have

been shown to be a functional module for nucleotide binding and hydrolysis (Tameling et al., 2002; Ueda et al., 2006). For I-2 it has been proposed that the ATP-bound state represents the active state and hydrolysis of the nucleotide is proposed to return the R protein into its resting state (Takken et al., 2006; Tameling et al., 2006). The nucleotide is likely bound at the interface between the NB, the ARC1 and ARC2, whose interactions are dependent on the nucleotide type (Takken et al., 2006).

Some aspects of the ARC1 subdomain function have been revealed by a series of domain swaps between R proteins Rx and Gpa2 (Rairdan and Moffett, 2006). These studies showed that the Rx ARC1 subdomain is necessary for the interaction of the N-terminus with the LRR domain. LRR binding seems to be a general feature of the ARC1 subdomain, since the Rx N-terminus was able to interact with the LRR domains of several other NB-LRR proteins. An extensive interaction surface with several individual contacts quantitatively contributing to the interaction was shown between the ARC1 and the LRR domain (Rairdan and Moffett, 2006). Together with the fact that no autoactive mutants have been described in this region suggests that the ARC1 subdomain is merely a scaffold regulating the intramolecular interactions with the LRR domain.

The ARC2 subdomain is proposed to relay pathogen recognition, mediated by the LRR domain into changes in R protein conformation, unleashing its downstream signaling potential. Swapping the Gpa2 ARC2 subdomain with the Rx ARC2 domain results in a constitutively active chimera (Rairdan and Moffett, 2006). Apparently, the ARC2 subdomain of Gpa2 and the LRR domain of Rx are sufficiently compatible to induce HR, but are not harmonized to prevent autoactivation. A role for the ARC2 subdomain in signal transduction fits with the fact that many autoactivating mutations in R proteins map to the ARC2 (Bendahmane et al., 2002; Shirano et al., 2002; de la Fuente van Bentem et al., 2005; Howles et al., 2005; Gabriëls et al., 2007). Support for such a regulatory function for the ARC2 is provided by mutational analysis of the conserved MHD motif in the ARC2 and modeling of the I-2 NB-ARC domain on the related human protein Apaf-1 (Chapter 3).

NB-LRR proteins can be roughly divided into two main subclasses depending on their N-terminal domain flanking the NB-ARC (Tameling and Takken, 2007; van Ooijen et al., 2007). This domain is either a region with homology to the *Drosophila* Toll and human Interleukin-1 Receptor proteins (the TIR domain), or a region of 120-200 amino acids without such homology, sometimes containing coiled-coil (CC) motifs. In solanaceous plants, several CC-NB-ARC-LRR proteins have a significantly larger N-terminal domain, and the presence of this extended N-terminus might indicate a difference in function between these and the ‘regular’ CC-NB-ARC-LRR proteins (Mucyn et al., 2006; Rairdan and Moffett, 2007). The R protein Mi-1.2

(Milligan et al., 1998; Vos et al., 1998) belongs to the group of CC-NB-ARC-LRR proteins with an extended N-terminus. Mi-1.2 responds to attempted host cell manipulation by three different root-knot nematode species (*Meloidogyne* spec.). In later studies, Mi-1.2 was also found to mediate resistance against infestations of phloem-feeding pests of white-fly and aphid (Martinez de Ilarduya et al., 2003; Nombela et al., 2003; Li et al., 2006). Mi-1.2 is member of a small gene family and is located in a cluster containing a paralogue (Mi-1.1) on chromosome 6. Mi-1.1 shares 91% amino-acid identity with Mi-1.2 (Milligan et al., 1998) and, like Mi-1.2, is transcribed although no known resistance specificity has been assigned to Mi-1.1. Numerous domain swaps have been made between Mi-1.1 and Mi-1.2 to generate genetic data on regions of the gene that are important for negative and positive regulation (Hwang et al., 2000; Hwang and Williamson, 2003).

Here, we address various aspects of the function of the Mi-1.2 NB-ARC subdomains in relation to its interaction with the LRR domain. Autoactivating mutants in the NB subdomain were found to be able to trigger HR upon co-expression of the separate CC-NB-ARC and LRR parts. In contrast, autoactivating mutations in the ARC2 subdomain fail to transcomplement and induce HR. These observations suggest that the ability to transcomplement depends on the NB-ARC subdomain affected by the mutation. In all combinations of CC-NB-ARC and LRR domains analysed, the physical interactions were not abolished, indicating that no gross changes in intramolecular interactions are associated with the induction of HR signalling. These results confirm a model suggesting a distinct functional role for each of the three NB-ARC subdomains. The NB subdomain is important for nucleotide binding and for the enzymatic activity of the NB-ARC domain, the ARC1 has a general LRR interacting role, and the ARC2 subdomain plays a dual regulatory role in sensing the nucleotide and translating pathogen perception into signalling.

Results

CC-NB-ARC and LRR expressed *in trans* complement to reconstitute a signalling-competent molecule

A chimaeric protein that consists of the CC-NB-ARC part of Mi-1.1 and the LRR domain of Mi-1.2 (referred to as Mi-DS4) induces a hypersensitive response (HR) upon transient expression in *Nicotiana benthamiana* leaves when expressed from the endogenous Mi-1.1 promoter (Hwang et al., 2000). Here we show that expression of this chimera Mi-DS4, but not Mi-1.1 or Mi-1.2, driven from the strong CaMV 35S promoter induces a strong necrosis 2 days after infiltration (Figure 1, left panel). This cell death is clearly visualised upon trypan blue staining of this leaf, to stain dead cells blue. Expression of Mi-1.1 or Mi-1.2 proteins induces a background level of cell

death visualised by a light blue hue upon trypan blue staining (Figure 1, right panel). To investigate the molecular basis behind the autoactive incompatibility between the Mi 1.1 CC-NB-ARC and Mi 1.2 LRR domains in Mi-DS4, and not for example in the reciprocal domain swap (referred to as Mi-DS2), functional complementation was analysed when the CC-NB-ARC and LRR domains were expressed *in trans*. To this end, the corresponding Mi-1.1 and Mi-1.2 parts were placed behind the 35S promoter and the four combinations were expressed in overlapping circles on *N. benthamiana* leaves by agroinfiltration. In this way the effect of expression of the separate domains, and combinations of two can be compared on a single leaf. In the infiltrated leafs depicted in Figure 2, the NB-ARC domains are expressed in the upper circles whereas the LRRs are expressed in the lower circles.

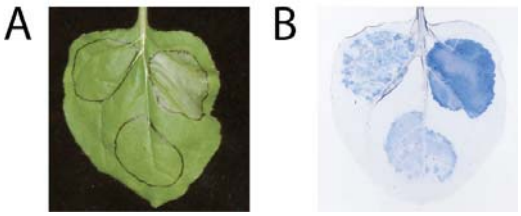

Figure 1
Mi-DS4 induces HR when expressed from the 35S promoter. *Nicotiana benthamiana* leaves were agroinfiltrated with constructs to express Mi-1.1, Mi-1.2 or Mi-DS4. A representative leaf was photographed two days after agroinfiltration (A). Cell death was visualised by trypan blue staining of the same leaf (B). Counter-clockwise, starting from top-left: Mi-1.1, Mi-1.2, and Mi-DS4.

Similar to the full-length proteins (Figure 1), HR signalling was initiated upon co-expression of Mi-1.1 CC-NB-ARC and Mi-1.2 LRR (overlapping region Figure 2B). To visualise the cell death the same leaves were stained with trypan blue (right panels in Figure 2). In contrast to Mi-DS4, the reconstituted Mi-1.1 (Figure 2A), Mi-DS2 (Figure 2C) or Mi-1.2 (Figure 2D) did not trigger HR. HR was also not observed in the non-overlapping regions, showing that expression of the separate CC-NB-ARC or LRR domain only induces a basal level of cell death. To be able to detect expression of the protein domains *in planta*, the Mi-DS4 constituents were fused to various tags at either their N- or C-terminus and analysed for functional transcomplementation. Of all combinations tested, only co-expression of non-tagged CC-NB-ARC protein and either non-tagged or N-terminally TAP-tagged LRR protein triggered HR. As the latter combination is still functional, we used it for all our transcomplementation assays (including Figure 2). These data show that we can functionally reconstitute an autoactivating Mi-1 chimaeric swap protein able to signal HR by expressing the Mi-1.1 CC-NB-ARC and Mi-1.2 LRR domains *in trans*. Because expression of the separate domains does not induce an HR, these data suggest that the two domains interact to activate defence signalling. The combination provides all positive

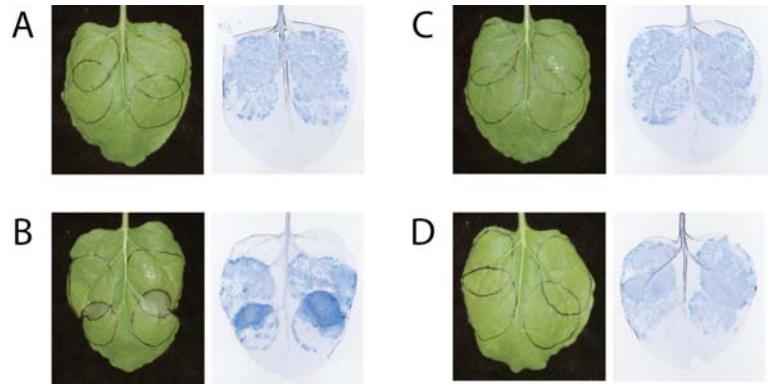

Figure 2

The Mi-DS4 phenotype can be reconstituted by co-expression of the CC-NB-ARC and LRR parts *in trans*. *N. benthamiana* leaves were agroinfiltrated with constructs to express the CC-NB-ARC or LRR domain of Mi-1.1 or Mi-1.2. Representative leaves were photographed two days after agroinfiltration. All infiltrations are performed in duplicate on the leaf halves. The top circles mark the regions of CC-NB-ARC infiltration and the bottom circles TAP-LRR infiltration. Cell death is visualised by trypan blue staining of the same leaf (right panel). **A)** Mi-1.1 CC-NB-ARC and Mi-1.1 TAP-LRR, **B)** Mi-1.1 CC-NB-ARC and Mi-1.2 TAP-LRR, **C)** Mi-1.2 CC-NB-ARC and Mi-1.1 TAP-LRR, **D)** Mi-1.2 CC-NB-ARC and Mi-1.2 TAP-LRR.

regulatory functions required to induce an HR, but lacks the negative regulation required to suppress this signalling in the absence of a pathogen.

Autoactivation in Mi-DS4 does not require dissociation of the LRR domain from the N-terminus

To analyse whether physical intramolecular interactions are responsible for the autoactivation phenotype of Mi-DS4, combinations of CC-NB-ARC and TAP-LRR constructs of Mi-1.1 and Mi-1.2 were co-expressed. On a Western blot of total protein lysates of the agroinfiltrated leaves, a band migrating at the expected size for the CC-NB-ARC protein (~100 kDa) is visualised (Figure 3, upper panel) using an Mi-1 antibody raised against the N-terminal region of Mi-1 not containing the LRR domain. The antibody also recognises the TAP-LRR fusion protein (~63 kDa) because of the general IgG-binding properties of the ProtA domain in the TAP tag.

To test physical interactions between the two protein domains, the TAP-LRR fusion protein was immunoprecipitated using agarose beads loaded with human IgG. Human IgGs were used to avoid cross-reactivity with the anti-rabbit secondary antibody needed for detection of the Mi-1 protein in subsequent immunoblots. The precipitated protein-complex was proteolytically cleaved from the beads using the specific TEV protease site in the TAP tag (Rohila et al., 2004). After pull-down, co-purification of CC-NB-ARC protein was analysed using the Mi-1 antibody (Figure 3, lower panel). Co-purification was found with all four combinations of Mi-1.1 and Mi-

1.2 domains. Apparently, the interaction of LRR domains with CC-NB-ARC is not restricted to their endogenous partners.

An interesting observation is co-precipitation of a band corresponding to the size of the TAP-LRR protein (63 kDa). As mentioned above, the Mi antibody does not recognise the cleaved non-tagged LRR domain and the ProtA epitope should remain bound to the beads. This observation suggests that either more than one LRR domain is present in one complex or that the conditions of the TEV protease cleavage are facilitating non-enzymatic dissociation of the complex from the beads. Since this phenomenon is not observed with other TAP-tagged proteins (data not shown), the latter hypothesis is unlikely. In any case, co-precipitation of CC-NB-ARC protein in the presence, and not in the absence of ,TAP-LRR protein shows that both are present in one complex and interaction is specific. This experiment clearly shows that a physical interaction is present in the transcomplementing Mi-DS4 combination. Based on the intensity of the bands the stoichiometry of the interaction is similar to that of the other combinations, implying that autoactivation does not require gross changes (i.e. dissociation) in intramolecular interactions between the N-terminus and the LRR domain.

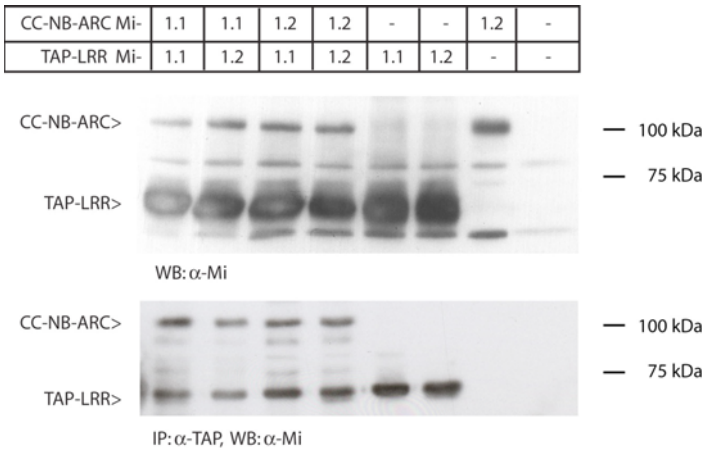

Figure 3

CC-NB-ARC and LRR domains of Mi-1.1 and Mi-1.2 physically interact when expressed *in trans. N. benthamiana* leaves were agroinfiltrated with constructs to express the domains of Mi-1.1 or Mi-1.2, as indicated in the heading. One day after agroinfiltration, protein extracts were made and subjected to immunoprecipitation using IgG-beads followed by immunoblotting and detection with αMi antibody. The upper panel represents an immunoblot of total protein extracts (input), the lower panel represents the TAP-precipitated protein complex after IP.

Identification of autoactivating mutations in the NB-ARC domain

The Mi-1.1 and Mi-1.2 proteins are 91% identical and the differences are scattered throughout the protein, making it difficult to pinpoint the residues responsible for

autoactivating incompatibilities. To be able to distinguish between positive and negative regulatory functions in the CC-NB-ARC and LRR combination, we focused on specific point mutations in the NB-ARC domain of Mi-1.2 that lead to autoactivation; T557S, H840A and D841V (Gabriëls et al., 2007; Chapter 3). Autoactivating mutants by definition represent HR signalling-competent molecules, in contrast to loss-of-function mutants that can be affected in various aspects of R protein function.

Autoactivating mutations in the NB-ARC domain map to the NB or to the ARC2 subdomain. The position of these mutations is visualised in a 3D model of the Mi-1.2 NB-ARC domain (Figure 4). This model is based on homology modelling of the Mi-1.2 NB-ARC on the crystal structure of the ADP-bound state of the NB-ARC domain of the human protein Apaf-1 (Riedl et al., 2005).

Based on this model, we selected two additional mutants. One of these represents a mutant in the NB subdomain (D630E) that maps to the Walker B motif (Fig. 4). The corresponding residue has also been shown to lead to autoactivation in I-2 (Tameling et al., 2006). The second mutant is a proposed loss-of-function mutant. In this double mutant (KT556/557AA), two highly conserved amino-acids in the nucleotide-binding P-loop are changed to alanine, thereby presumably abolishing the ability to bind nucleotides (Fig. 4). As can be clearly seen in the 3D model, all mutations used in this study cluster at the nucleotide-binding interface, showing that, although the mutations map to different regions in a linear sequence, they cluster spatially.

Mutations in the ARC2, but not in the NB subdomain, abolish transcomplementation

To compare the extend of cell death mediated by the five Mi-1.2 NB-ARC mutants, they were transiently expressed in *N. benthamiana* leaves using agroinfiltration. Figure 5 shows the infiltrated leafs two days after infiltration. At this time-point, the ARC2 mutants H840A (bottom left) and D841V (top right) induced a clear HR, whereas the NB mutants T557S (bottom right) and D630E (middle right) do not yet induce a specific cell death response. The T557S initiated HR becomes apparent after 3 days (Gabriëls et al., 2007), whereas the D630E mutation leads to visual necrosis 5 days after infiltration (data not shown). Of the four autoactivating mutants, H840A and D841V are the fastest, whereas the two NB mutants (T557S and D630E) induce a relatively slow HR, not observed with wild-type Mi-1.2 or with the KT556/557AA mutant.

To test whether transcomplementation of CC-NB-ARC and LRR domains is affected in any of these NB-ARC mutants, we co-expressed wild-type and the five mutant CC-NB-ARC proteins and wild-type TAP-LRR protein in overlapping circles in *N. benthamiana* leaves. In all leaves pictured in Figure 6, the NB-ARC domains are

infiltrated in the upper circle and the lower circle represent the region of Mi-1.2 TAP-LRR expression. As expected, the wild-type (Fig. 6A) and predicted loss-of-function KT556/557AA (Fig. 6B) NB-ARC domains did not induce HR when co-expressed with the LRR domain. The absence of HR was verified by trypan blue staining of the same leaves (right panels).

The NB mutants T557S and D630E did transcomplement and reconstituted autoactivity (overlapping zone in Fig. 6C and D). Similar as the full-length protein, the D630E mutant induced a milder response than the T557S mutant, but HR was clearly visible in the overlapping region upon trypan blue staining (Figure 6D, right panel). These results show that NB subdomain mutants are able to induce HR when the LRR domain is expressed *in trans*. The cell death response is faster than that induced by the full-length protein, presumably due to the higher expression levels observed for the separate domains (data not shown).

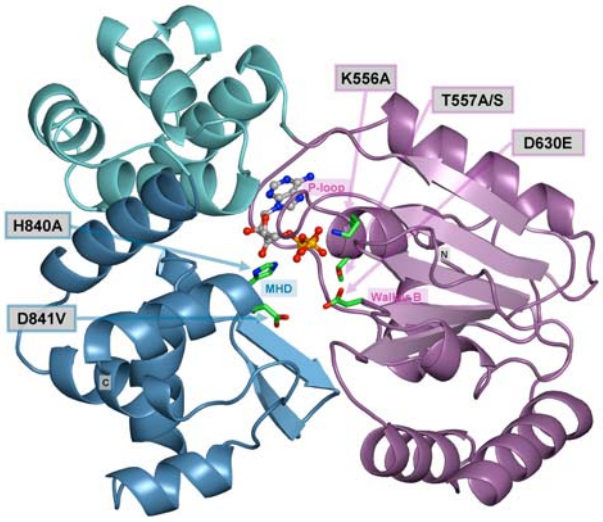

Figure 4

Structure model of the Mi-1.2 NB-ARC domain. The model was created using the ADP bound structure of human Apaf-1 (PDB code 1z6t, chain A) as structural template. The positions of the P-loop, the Walker B motif, and the MHD motif are indicated. Arrows point to the locations of Mi-1.2 mutant residues used in this study. They are represented as sticks, whereas ADP atoms are depicted as balls-and-sticks. Subdomain colouring is as follows: NB: pink, ARC1: green, ARC2: blue.

In contrast to the NB mutants, co-expression of CC-NB-ARC variants containing the strong ARC2 autoactivation mutants H840A or D841V reproducibly fails to induce HR responses (Figure 6E and F). Apparently, the mutations that result in the strongest autoactivation phenotypes *in cis* (Figure 5) cannot complement with the LRR domain to reconstitute a functional molecule when expressed *in trans* (Figure 6). These results show that functional transcomplementation of autoactivity depends on the subdomain of the NB-ARC that is affected.

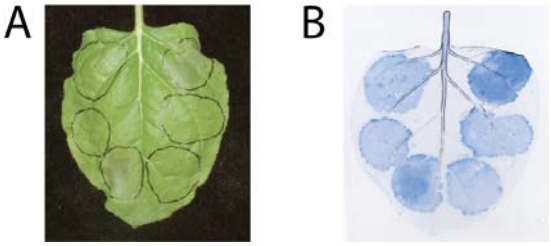

Figure 5
Specific point mutations in the Mi-1.2 NB-ARC domain result in autoactivity. *Nicotiana benthamiana* leaves were agroinfiltrated with constructs to express Mi-1.2 proteins mutated in the NB-ARC domain. A picture of a representative leaf was taken three days after agroinfiltration (A). Cell death is visualised by trypan blue staining of the same leaf (B). Counter-clockwise, starting from top-left: wild-type, KT556/557AA, H840A, T557S, D630E, D841V

Mutations in the NB-ARC domain do not lead to dissociation of the LRR domain

To investigate whether the observed differences in the transcomplementation assay can be explained by a change in physical interaction of CC-NB-ARC and LRR, combinations of mutant CC-NB-ARC and TAP-LRR proteins were co-expressed. The Western blot of the total protein lysates (Figure 7, upper panel) shows equal

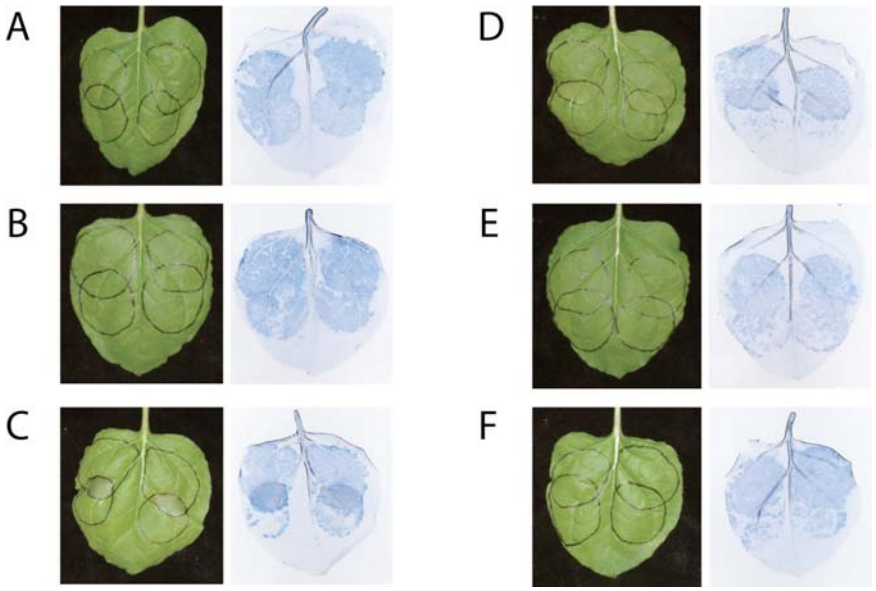

Figure 6
Transcomplementation of Mi-1.2 NB-ARC mutants depends on which subdomain is affected. *N. benthamiana* leaves were agroinfiltrated with constructs to express CC-NB-ARC (mutants) or the LRR domain of Mi-1.2. Representative leaves were photographed two days after agroinfiltration. On each leaf, duplicates are infiltrated on the leaf halves. The top circles mark the regions of (mutant) Mi-1.2 CC-NB-ARC expression and the bottom circles of Mi-1.2 TAP-LRR expression. Cell death was visualised by trypan blue staining of the same leaf (right panel). CC-NB-ARC variants: **A)** wild-type, **B)** KT556/557AA, **C)** T557S, **D)** D630E, **E)** H840A, **F)** D841A.

expression of the CC-NB-ARC variants and of the Mi-1.2 TAP-LRR proteins. Both migrate according to their predicted masses of ~100 and 63 kDa.

The Mi-1 protein-complex was precipitated using human IgG-beads and released using TEV protease. Co-precipitation of CC-NB-ARC domains with TAP-LRR was analysed on Western blots using the Mi-1 antibody. As can be seen in the lower panel of Figure 7, all CC-NB-ARC variants tested interact equally well with the Mi-1.2 LRR domain. These interactions show that even though transcomplementation of the CC-NB-ARC and LRR domains depends on the location of mutations in the NB and ARC2 subdomains, there are no detectable changes in intramolecular interactions in these mutants. Apparently, interaction of the LRR domain with its N-terminus does not depend on the functionality of the combination, and is not sufficient for autoactivation.

Discussion

We have adressed the molecular background of autoactivating domain swaps of the Mi-1.2 and Mi-1.1 proteins, and of autoactivating and loss-of-function point mutations in the NB-ARC domain of Mi-1.2, summarised in Table 1. Using an Mi-1 antibody and a tagged LRR construct, we have been able to study intramolecular interaction of the LRR domain and the CC-NB-ARC part of Mi-1 paralogues and NB-ARC mutants. The set of mutants depicted in the model in Figure 4 enabled us to investigate the effect of mutations in NB-ARC subdomains on transcomplementation and intramolecular interaction with the LRR domain. In all combinations of Mi-1 LRR and CC-NB-ARC variants, a physical interaction was observed. Apparently, autoactivation and loss-of-function mutations in NB and ARC2 studied here do not result in dissociation of the CC-NB-ARC and LRR domains. The ability to transcomplement, however, was found to be dependent on the NB-ARC subdomain affected by the autoactivating mutation.

The observed constitutive interaction between the CC-NB-ARC and LRR domain appears to contrasts with a previously proposed model based on genetic data and domain swap analyses (e.g. for Mi-DS4) that suggest dissociation of these domains upon (auto)activation (Hwang et al., 2000; Hwang and Williamson, 2003). However, it is likely that the functional interaction between these two domains is lost, even though the physical interactions remain. The observed interactions of the LRR domain with the CC-NB-ARC parts in Mi-DS4, Mi-DS2, and both wild-type proteins show that association of the LRR domain with the N-terminus is not sufficient to induce HR, nor to repress it. Since Mi-1.1 and Mi-DS2 failed to confer nematode resistance (Hwang et al., 2000), the combination of the genuine CC-NB-ARC and LRR (Mi-1.2) domains is required to perceive the nematode-derived stimulus and trigger defence.

To explain how the point mutants in the NB-ARC affect the activation state, the NB-ARC domain of Mi-1.2 was modelled on the APAF-1 template (Figure 4). The replacement of the highly conserved lysine (K556) and threonine (T557) in the P-loop of the NB subdomain to alanine is predicted to disrupt nucleotide binding. In the structure of Apaf-1, the P-loop provides 7 of the 8 direct hydrogen bonds to the bound ADP (the 8th is provided by the histidine in the MHD motif) (Riedl et al., 2005), showing the importance of this motif for nucleotide binding. Direct support for a role in nucleotide binding by the P-loop in R proteins is provided by the observation that replacement of the corresponding lysine in I-2 results in a nucleotide binding mutant with a loss-of-function phenotype (Tameling et al., 2002). The T557S mutation in the

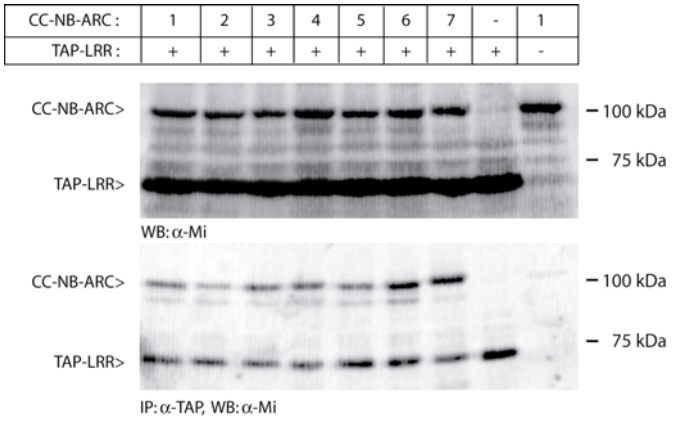

Figure 7

Mi-1.2 CC-NB-ARC mutant variants interact with the LRR domain. *N. benthamiana* leaves were agroinfiltrated with constructs to express parts of (mutant) Mi-1.2 or Mi-1.1. One day after agroinfiltration, protein extracts were made and subjected to immunoprecipitation using IgG-beads followed by immunoblotting and detection using αMi antibody. The upper panel shows an immunoblot of total protein extracts (input), the lower panel represents the precipitated protein complex after IP. In this experiment, Mi-1.2 TAP-LRR was expressed in combination with variant CC-NB-ARC constructs, as indicated in the heading. CC-NB-ARC numbering: 1: wild-type Mi-1.2, 2: KT556/557AA, 3: T557S, 4: D630E, 5: D841V, 6: H840A, 7: wild-type Mi-1.1.

P-loop of Mi-1.2 apparently does not abolish nucleotide binding, since this mutant has an autoactivation phenotype. Possibly, the orientation of the bound nucleotide is aberrant in this mutant and mimics the activated state, or, alternatively, the mutation reduces the ATPase activity. The latter hypothesis is supported by analysis of two autoactivation mutations in the NB subdomain of I-2 that were shown to have a reduced hydrolysis capacity (Tameling et al., 2006). One of them is the D283E mutation in the Walker B motif. This acidic residue is thought to be a catalytic base that is required for ATP hydrolysis by P-loop ATPases (Leipe et al., 2004). Based on the structural conservation, we therefore propose the same role for the analogous D630E mutation in Mi-1.2 and predict that it will be a hydrolysis mutant. The

autoactivating phenotypes observed upon mutation of the MHD motif in the ARC2 are likely based on a destabilised interaction between this domain and the nucleotide. A CC-NB-ARC domain harbouring an autoactivating mutation in the MHD motif is not able to induce an HR on itself (Figure 2 and 6), but requires the LRR domain *in cis* (Figure 5). When these domains are expressed *in trans*, HR signalling is not induced although their interaction is not compromised. Apparently, the positive regulatory function of the LRR on the CC-NB-ARC domain, required for the protein to activate defence signalling, is lost when presented *in trans*. We can exclude that the separated LRR domain exhibits dominant negative regulation of the MHD mutants, since co-expression of the LRR with full-length MHD mutants does not suppress HR. These observations suggest a sensory and regulatory role for the ARC2 subdomain in mediating LRR-derived signals.

In Rx, the corresponding MHD mutant D460V can still transcomplement with the LRR domain (Moffett et al., 2002). A possible basis for this difference is that Rx belongs to a different group of CC-NB-ARC-LRR proteins. It would be interesting to examine whether the ability to transcomplement the MHD mutant phenotype is NB-LRR (sub)class-specific.

To summarize, this study provides the first data on intramolecular interaction between domains of an NB-LRR R protein with an extended CC domain. The robust interaction between LRR and CC-NB-ARC domains supports the hypothesis by Rairdan et al., 2007, that the responsible interface consists of several contact points and can therefore not readily be disturbed. Our results support a distinct role for the three NB-ARC subdomains. The NB subdomain is involved in nucleotide binding and hydrolysis, and mutations that disrupt binding result in a loss of function phenotype whereas putative hydrolysis mutants are autoactivating (Figure 5). Autoactivity conferred by NB subdomain mutants is presumably caused by a shift in the equilibrium towards the ATP-bound state, which is proposed to be the active state (Tameling et al., 2006). In the NB subdomain mutants, the negative regulation exerted by the LRR is lost, but the positive regulatory functions are required and sufficient to confer the autoactivation phenotype (Figure 6). In contrast, mutation of the ARC2 also alleviates negative regulation, but the positive regulation of the LRR domain can only be provided *in cis* (Figure 5) and not *in trans* (Figure 6), suggesting that the interaction between these domains is altered even though interaction is not lost (Figure 7). Binding to the LRR is therefore likely to be mediated by the ARC1 subdomain, in accordance to the observations described for Rx (Rairdan and Moffett, 2006).

Altogether, our data support a model in which perception of a pathogen-derived factor by the LRR domain results in an alteration of the interaction interface between the LRR domain and the ARC2 subdomain, resulting in a release of the negative

regulation exerted by the LRR on the NB-ARC domain and transition to the activated state.

Further studies will be required to understand how positive and negative regulation by the LRR on the NB-ARC domain is executed. However, the analysis of intramolecular interactions aid to reveal parts of the basic mechanisms underlying activation. To fully understand the molecular dynamics of the interactions, crystal structures of full-length R proteins in the ATP- and ADP-bound state will be essential. Changes in conformation might be subtle and rather than complete association or dissociation of (sub)domains, intricate changes in binding interfaces might be sufficient to unleash the signalling potential of an R protein.

Acknowledgements

We like to thank Harold Lemereis for plant handling. We are grateful to Valerie Williamson for providing us with the Mi-DS4 construct and helpful discussions. G.v.O. is supported by the Research Council for Earth and Life Sciences (ALW) with financial aid from the Netherlands Organization for Scientific Research (NWO). G.M. and M.A. have been financially supported by the German National Genome Research Network (NGFN). The research has been conducted in the context of the BioSapiens Network of Excellence funded by the European Commission under grant number LSHG-CT-2003-503265.

Materials and methods

Construction of binary vectors

All PCR primers used in this study (marked FPxxx) were purchased from MWG (Germany), and are listed in Table 2. Construction of a binary vector expressing Mi-1.2 (pG74) was described elsewhere (Gabriëls et al., 2007). Mi-1.1 was amplified from plasmid G3 (Keygene N.V.) with primers FP764 and FP766. Gateway *att*B flanks were added by adapter PCR using primers FP872 and FP873. The PCR product was transferred via entry clone pDONR207 (Invitrogen) to binary vector CTAPi (Rohila et al., 2004) by the Gateway one-tube protocol for cloning *att*B-PCR products directly into destination vectors (Invitrogen). In the same way, Mi-DS4 was amplified from plasmid Mi-DS4 (Hwang et al., 2000) and cloned into CTAPi. Note that the endogenous stop codon remains present in these constructs, so there is no translational fusion to the TAP tag. Constructs expressing the Mi-1.2 mutants T557S, H840A and D841V have been described elsewhere (Gabriëls et al., 2007; van Ooijen et al., submitted). D630E was generated by overlap extension PCR using primer sets FP554/FP212 and FP182/FP555 on template pSE23 (Gabriëls et al., 2007). The 1330 and 260 bp pcr products were joined in a second amplification step using FP182/FP212. A 325 bp restriction fragment generated with *Age*I and *Xho*I containing the desired mutation was used to replace the wildtype sequence in pSE23 to obtain pG23. The full length Mi-1.2 D630E sequence was amplified using FP764 and FP766, Gateway *att*B sites were added with FP872 and FP873 and the resulting fragment was transferred to binary vector CTAPi as described above. The Mi-1.2 KT556/557AA

T2	Oligonucleotides used in this study
FP	Sequence
182	ggggtacccggctatttctttaccgacatc
212	catgccatggccgagctagatgaggatgaac
554	gtcttagatgaagtgtgggatac
555	gtatcccacacttcatctaagac
764	aaaaagcaggctctatggaaaaacgaaaagatatt
766	agaaagctgggttctacttaaataaggggatattctt
857	aaaaagcaggctctggtaaacacctctattctttg
859	agaaagctgggttctaagaatgccttttcttatttgaa
872	ggggacaagtttgtacaaaaaagcaggct
873	ggggaccactttgtacaagaaagctgggt
1099	gtatgccgggttcaggtgcagcaactttggcatacaaagtatac
1102	gtatactttgtatgccaaagttgctgcacctgaacccggcatac

construct was generated by circular mutagenesis (Hemsley et al., 1989) on template pG104 (van Ooijen et al., submitted) using FP1099/FP1102 to obtain pG108. An *Eco*72I/*Bsp*119I restriction fragment carrying the mutation was exchanged with that in pG74 to obtain Mi-1.2 KT556/557AA. Mi-1.1 and Mi-1.2 LRR sequences (residues 1-899) were amplified from G3 and pKG6210 (Keygene N.V.), respectively, using primers FP857 and FP766. Gateway *att*B flanks were added using FP872 and FP873 and the fragment was transferred to pDONR207 by a Gateway BP reaction (Invitrogen) and subsequently to NTAPi (Rohila et al., 2004) to obtain N-terminally TAP tagged LRR domains. All CC-NB-ARC (residues 900-1258) constructs were generated by the Gateway one-tube protocol for cloning *att*B fragments directly in destination vectors (Invitrogen). Primers FP764 and FP859 were used on PCR templates pKG6210 (Mi-1.2, Keygene N.V.) and G3 (Mi-1.1, Keygene N.V.), or the full-length clones of the Mi-1.2 mutants described above and in (Gabriëls et al., 2007; van Ooijen et al., submitted). Note that a stop codon has been incorporated in the reverse primer to prevent translational fusion to the TAP tag in these CC-NB-ARC constructs.

***Agrobacterium*-mediated transient transformation**

A. tumefaciens strain GV3101(pMP90) (Koncz and Schell, 1986) was transformed with binary constructs (Takken et al., 2000) and grown to OD_{600}=0.8 in LB-Mannitol (10g/l tryptone, 5 g/l yeast extract, 2.5 g/l NaCl, 10 g/l mannitol) medium supplemented with 20 µM acetosyringone and 10 mM MES pH 5.6. Cells were pelleted and resuspended in infiltration medium (1x MS salts, 10 mM MES pH 5.6, 2% w/v sucrose, 200 µM acetosyringone) and infiltrated at OD_{600}=0.2 (for LRR constructs) or 1 (for full-length or CC-NB-ARC constructs) into four- to five-week-old *N. benthamiana* leaves.

Protein extraction, immunoprecipitation and Western blotting

Infiltrated leaves were harvested and pooled 24 hours after agroinfiltration and frozen in liquid nitrogen. After grinding the tissue, it was allowed to thaw in 2 ml protein extraction buffer per gram of tissue (25 mM Tris pH 8, 1 mM EDTA, 150 mM NaCl, 5 mM DTT, 0,1% NP-40, 1 x Roche Complete protease inhibitor cocktail and 2% Poly-(Vinyl-Poly-Pyrolidone)). Extracts were centrifuged at 12,000 krcf at 4º C for 10 minutes and the supernatant was passed over 4 layers of Miracloth to obtain a total protein lysate. 1 ml of total protein lysate was incubated with 20 µl human IgG-agarose beads (Sigma) rotating head-over-head at 4º C for 1 hour. Beads with bound protein complexes were pelleted at 2,000 rpm for 10 seconds and washed 4 times with 1 ml ice-cold TEV cleavage buffer (10 mM Tris pH 8, 150 mM NaCl, 0.5 mM EDTA, 0.1% NP-40 and 1 mM DTT). 100 µl TEV cleavage buffer and 10 units recombinant AcTEV protease (Invitrogen) were added to the pelleted beads and the proteolytic reaction was carried out shaking vigorously for 1.5 hours at 16º C. The supernatant was mixed with Laemmli sample buffer, run on 8% SDS-PAGE gels and blotted on PVDF membranes using semi-dry blotting. 5% skimmed milk powder was used as blocking agent. As a primary antibody, a 1:4000 dilution of the Mi-1 antibody (van Ooijen et al., submitted) was used and as a secondary antibody a 1:4000 dilution of goat-anti-rabbit linked to either horseradish peroxidase (Figure 3) or alkaline phosphatase (Figure 8). The signal was visualised by

measuring either luminescence (ECL and BioMax MR film (Kodak) Figure 3) or fluorescence (ECF and detection by phospho-imager (STORM), Figure 8).

3D structure model of the Mi-1.2 NB-ARC domain

A pairwise sequence-structure alignment of tomato R protein Mi-1.2 and human Apaf-1 was constructed based on the multiple alignment of R protein NB-ARC domains described in (van Ooijen et al., submitted). The 3D-modeling server WHAT IF (Vriend, 1990) returned a full-atom structure model of the NB-ARC domain of Mi-1.2. The structure of Apaf-1 (PDB code 1z6t, chain A) comprises the residues 108-450 (UniProt sequence O14727) and is mapped onto Mi-1.2 residues 505-852 (UniProt sequence O81137). The protein structure image of the model was illustrated using PyMOL (http://www.pymol.org).

References

Ade, J., DeYoung, B.J., Golstein, C., and Innes, R.W. (2007). Indirect activation of a plant nucleotide binding site-leucine-rich repeat protein by a bacterial protease. Proc Natl Acad Sci USA **104**, 2531-2536.

Albrecht, M., and Takken, F.L.W. (2006). Update on the domain architectures of NLRs and R proteins. Biochem Biophys Res Commun **339,** 459-462.

Bendahmane, A., Farnham, G., Moffett, P., and Baulcombe, D.C. (2002). Constitutive gain-of-function mutants in a nucleotide binding site-leucine rich repeat protein encoded at the *Rx* locus of potato. Plant J **32,** 195-204.

de la Fuente van Bentem, S., Vossen, J.H., de Vries, K.J., van Wees, S., Tameling, W.I.L., Dekker, H.L., de Koster, C.G., Haring, M.A., Takken, F.L.W., and Cornelissen, B.J.C. (2005). Heat shock protein 90 and its co-chaperone protein phosphatase 5 interact with distinct regions of the tomato I-2 disease resistance protein. Plant J **43,** 284-298.

Gabriëls, S.H.E.J., Vossen, J.H., Ekengren, S.K., van Ooijen, G., Abd-El-Haliem, A.M., van den Berg, G.C.M., Rainey, D.Y., Martin, G.B., Takken, F.L.W., de Wit, P.J.G.M., and Joosten, M.H.A.J. (2007). An NB-LRR protein required for HR signalling mediated by both extra- and intracellular resistance proteins. Plant J **50,** 14-28.

Hemsley, A., Arnheim, N., Toney, M.D., Cortopassi, G., and Galas, D.J. (1989). A simple method for site-directed mutagenesis using the polymerase chain reaction. Nuc Acids Res **17,** 6545-6551.

Howles, P., Lawrence, G., Finnegan, J., McFadden, H., Ayliffe, M., Dodds, P., and Ellis, J. (2005). Autoactive alleles of the flax *L6* rust resistance gene induce non-race-specific rust resistance associated with the hypersensitive response. Mol Plant Microbe Interact **18,** 570-582.

Hwang, C.F., and Williamson, V.M. (2003). Leucine-rich repeat-mediated intramolecular interactions in nematode recognition and cell death signaling by the tomato resistance protein Mi. Plant J **34,** 585-593.

Hwang, C.F., Bhakta, A.V., Truesdell, G.M., Pudlo, W.M., and Williamson, V.M. (2000). Evidence for a role of the N terminus and leucine-rich repeat region of the *Mi* gene product in regulation of localized cell death. Plant Cell **12,** 1319-1329.

Koncz, C., and Schell, J. (1986). The promoter of Tl-DNA gene *5* controls the tissue-specific expression of chimaeric genes carried by a novel type of *Agrobacterium* binary vector. Mol Gen Genet **204,** 383-396.

Leipe, D.D., Koonin, E.V., and Aravind, L. (2004). STAND, a class of P-loop NTPases including animal and plant regulators of programmed cell death: multiple, complex domain architectures, unusual phyletic patterns, and evolution by horizontal gene transfer. J Mol Biol **343,** 1-28.

Leister, R.T., Dahlbeck, D., Day, B., Li, Y., Chesnokova, O., and Staskawicz, B.J. (2005). Molecular genetic evidence for the role of *SGT1* in the intramolecular complementation of Bs2 protein activity in *Nicotiana benthamiana*. Plant Cell **17,** 1268-1278.

Li, Q., Xie, Q.G., Smith-Becker, J., Navarre, D.A., and Kaloshian, I. (2006). Mi-1-Mediated aphid resistance involves salicylic acid and mitogen-activated protein kinase signaling cascades. Mol Plant Microbe Interact **19,** 655-664.

Martinez de Ilarduya, O., Xie, Q., and Kaloshian, I. (2003). Aphid-induced defense responses in Mi-1-mediated compatible and incompatible tomato interactions. Mol Plant Microbe Interact **16,** 699-708.

Milligan, S.B., Bodeau, J., Yaghoobi, J., Kaloshian, I., Zabel, P., and Williamson, V.M. (1998). The root knot nematode resistance gene *Mi* from tomato is a member of the leucine zipper, nucleotide binding, leucine-rich repeat family of plant genes. Plant Cell **10,** 1307-1319.

Moffett, P., Farnham, G., Peart, J., and Baulcombe, D.C. (2002). Interaction between domains of a plant NBS-LRR protein in disease resistance-related cell death. EMBO J **21,** 4511-4519.

Mucyn, T.S., Clemente, A., Andriotis, V.M.E., Balmuth, A.L., Oldroyd, G.E.D., Staskawicz, B.J., and Rathjen, J.P. (2006). The tomato NBARC-LRR protein Prf Interacts with Pto kinase in vivo to regulate specific plant immunity. Plant Cell. **18**, 2792-2808.

Nombela, G., Williamson, V.M., and Muniz, M. (2003). The root-knot nematode resistance gene Mi-1.2 of tomato is responsible for resistance against the whitefly *Bemisia tabaci*. Mol Plant Microbe Interact **16,** 645-649.

Rairdan, G., and Moffett, P. (2007). Brothers in arms? Common and contrasting themes in pathogen perception by plant NB-LRR and animal NACHT-LRR proteins. Microbes Infect **9,** 677-686.

Rairdan, G.J., and Moffett, P. (2006). Distinct domains in the ARC region of the potato resistance protein Rx mediate LRR binding and inhibition of activation. Plant Cell **18,** 2082-2093.

Rathjen, J.P., and Moffett, P. (2003). Early signal transduction events in specific plant disease resistance. Curr Opin Plant Biol **6,** 300-306.

Riedl, S.J., Li, W., Chao, Y., Schwarzenbacher, R., and Shi, Y. (2005). Structure of the apoptotic protease-activating factor 1 bound to ADP. Nature **434,** 926-933.

Rohila, J.S., Chen, M., Cerny, R., and Fromm, M.E. (2004). Improved tandem affinity purification tag and methods for isolation of protein heterocomplexes from plants. Plant J **38,** 172-181.

Shirano, Y., Kachroo, P., Shah, J., and Klessig, D.F. (2002). A gain-of-function mutation in an *Arabidopsis* Toll Interleukin1 receptor-nucleotide binding site-leucine-rich repeat type R gene triggers defense responses and results in enhanced disease resistance. Plant Cell **14,** 3149-3162.

Sun, Q., Collins, N.C., Ayliffe, M., Smith, S.M., Drake, J., Pryor, T., and Hulbert, S.H. (2001). Recombination between paralogueues at the *rp1* rust resistance locus in maize. Genetics **158,** 423-438.

Takken, F.L.W., Albrecht, M., and Tameling, W.I.L. (2006). Resistance proteins: molecular switches of plant defence. Curr Opin Plant Biol **9,** 383-390.

Takken, F.L.W., Luderer, R., Gabriëls, S.H.E.J., Westerink, N., Lu, R., de Wit, P.J.G.M., and Joosten, M.H.A.J. (2000). A functional cloning strategy, based on a binary PVX-expression vector, to isolate HR-inducing cDNAs of plant pathogens. Plant J **24,** 275-283.

Tameling, W.I.L., and Takken, F.L.W. (2007). Resistance proteins: scouts of the plant innate immune system. Eur J Plant Pathol **121,** 243-255

Tameling, W.I.L., Elzinga, S.D., Darmin, P.S., Vossen, J.H., Takken, F.L.W., Haring, M.A., and Cornelissen, B.J.C. (2002). The tomato *R* gene products I-2 and Mi-1 are functional ATP binding proteins with ATPase activity. Plant Cell **14,** 2929-2939.

Tameling, W.I.L., Vossen, J.H., Albrecht, M., Lengauer, T., Berden, J.A., Haring, M.A., Cornelissen, B.J.C., and Takken, F.L.W. (2006). Mutations in the NB-ARC domain of I-2 that impair ATP hydrolysis cause autoactivation. Plant Physiol **140,** 1233-1245.

Ueda, H., Yamaguchi, Y., and Sano, H. (2006). Direct interaction between the tobacco mosaic virus helicase domain and the ATP-bound resistance protein, N factor during the hypersensitive response in tobacco plants. Plant Mol Biol **61,** 31-45.

van Ooijen, G., van den Burg, H.A., Cornelissen, B.J.C., and Takken, F.L.W. (2007). Structure and function of resistance proteins in solanaceous plants. Annu Rev Phytopathol **45,** 43-72.

Vos, P., Simons, G., Jesse, T., Wijbrandi, J., Heinen, L., Hogers, R., Frijters, A., Groenendijk, J., Diergaarde, P., Reijans, M., Fierens Onstenk, J., De Both, M., Peleman, J., Liharska, T., Hontelez, J., and Zabeau, M. (1998). The tomato *Mi-1* gene confers resistance to both root-knot nematodes and potato aphids. Nature Biotech **16,** 1365-1369.

Vriend, G. (1990). WHAT IF: a molecular modeling and drug design program. J Mol Graph **8,** 52-56, 29.

Xing, W., Zou, Y., Liu, Q., Liu, J., Luo, X., Huang, Q., Chen, S., Zhu, L., Bi, R., Hao, Q., Wu, J.W., Zhou, J.M., and Chai, J. (2007). The structural basis for activation of plant immunity by bacterial effector protein AvrPto. Nature **449,** 243-247.

Yan, N., Chai, J., Lee, E.S., Gu, L., Liu, Q., He, J., Wu, J.W., Kokel, D., Li, H., Hao, Q., Xue, D., and Shi, Y. (2005). Structure of the CED-4-CED-9 complex provides insights into programmed cell death in *Caenorhabditis elegans*. Nature **437,** 831-837.